Modelling, Design and Development of Tissue mimicking phantoms for Ultrasound Elastography

M.Kavitha[1], M.Ramasubba Reddy[2]
Biomedical Engineering Division, Department of Applied Mechanics
Indian Institute of Technology Madras
Chennai, 600036, India
Email: kavitharunkumar@gmail.com[1], rsreddy@iitm.ac.in[2]

S.Suresh[3]
Mediscan Systems
Chennai, 600040, India
Email: mediscan@gmail.com[3]

***Abstract*—Modelling of tissue mimicking phantoms play a crucial role in the development of Ultrasound Elastography. This paper deals with both computer modelling and physical design of agar based tissue mimicking phantoms with embedded inclusions of varying stiffness in uniform homogeneous background. The elastic properties of agar based phantom are imaged using Ultrasound Elastography. The computer modelling and linear strain analysis of the phantom are done using finite element method. The visual display of strain results are compared with the experimental results and they are in good agreement. This allows us to model many hypothetical structures of real life and will be useful while validating signal processing algorithms for new imaging modalities.**

Keywords- tissue mimicking phantoms; modelling and simulation; ultrasound elastography; finite element analysis; agar based composite phantoms.

I. Introduction

Pathological changes in soft tissues are often correlated with changes in the tissue mechanical properties, such as the elastic modulus [1]. In many cases, these pathological changes do not alter the echogenicity of the tissue and may go undetected in normal B-mode Ultrasound Imaging. However these may be detected by imaging the elastic properties of tissue. The elastic properties are described as measure of material's resistance to deformation, in compression/tension (Young's modulus, E) and in shear (shear modulus, μ) [2]. Tissue elastic properties are measured using ultrasound by a method known as Ultrasound Elastography (UE). It involves acquiring ultrasound signals from tissues before and after a small static external compression [3]. The displacement or strain produced inside the tissue due to the compression is measured and displayed as an Elastogram.

Being a new technique, Ultrasound Elastography imaging needs thorough evaluation in data acquisition, image contrast and patient safety. Such calibration is a time consuming process, biological tissues can not be used in that situation since they lose their properties with time after harvesting from human body. This leads to the necessity of simulation models and tissue mimicking phantoms. Phantoms are inanimate objects designed to match the tissue properties with variations to cover both normal and abnormal tissues modelled either by a software program or physically by a gel.

Computer models of tissue mimicking phantoms can be created using finite element software packages. It enables us to predict the mechanical behaviour of the tissues under compression at every point of location which in turn will give ideal strain image. From these ideal images, we can learn what we can expect from real clinical cases and helps us to optimize the signal and image processing algorithms.

In this work, computer phantoms are made and analysed with various concentration of agar using finite element analysis. The physical composite phantoms using agar are also developed and strain images are taken using Ultrasound Elastography machine. The simulation results are compared with the experimental images.

II. Materials and Methods

A. Modelling of human soft tissue- Theory

Human soft tissue exhibits anisotropic, non-linear and visco elastic behaviour [1] where the stress and strain are time dependant. Therefore an exact modelling of the mechanical behaviour of the tissue under loading is difficult and cumbersome. Such materials when they are subjected to loading, show truly elastic deformation only under certain assumptions. The first assumption is that tissue is an elastic material showing one to one relationship between stress and strain. Even after, the general behaviour of the tissue is still non linear with an exponential stress strain relationship. However when strain is small, typically less than 10%, the exponential relationship can be approximated by a linear one. When these conditions are met, the strain and stress are not dependent on loading rate and when the load is removed, the material returns quickly to its original pre-deformed configuration. In such cases, the elastic body stress σ_{ij} is related to strain ϵ_{kl} through

$$\sigma_{ij} = C_{ijkl}\ \epsilon_{kl} \tag{1}$$

The above equation is the generalized form of the Hookes law which establishes the linear relationship between the components of the stress and the components of the strain at any point in the body through the material property tensor, C_{ijkl}. The subscripts i, j, k and l vary from 1 to 3 for a 3-d object. C_{ijkl} is a 4th order tensor and is known as the elastic constants of the material. A full description of the material without any further simplifying assumptions require altogether 81 elastic constants. We now bring forth our simplifying

978-1-4673-1666-8/12/$31.00 ©2012 IEEE

assumptions linear elastic isotropic, which are assumed to be valid for human soft tissue, the elastic components are reduced to just two which are termed as the Lame parameters λ and μ. The Lame parameters λ and μ are seldom used to describe the material properties under these assumptions. Instead, Young's modulus (E) and Poisson's ratio (ν) which are related to λ and μ can be used. It can easily be shown that for a uni axial compressive loading which produces a compressive stress σ and strain ϵ, the Young's modulus is

$$E = \frac{\sigma}{\epsilon} = \frac{\mu(3\lambda + 2\mu)}{\lambda + \mu} \tag{2}$$

Another important parameter derivable from Hooke's law is the Poisson's ratio ν which is defined as a measure of the transverse strain resulting from an axial strain due to compression. It is given as

$$\nu = \frac{\lambda}{2(\lambda + \mu)} \tag{3}$$

Assuming that these tissues mainly consist of water, which is incompressible with a Poisson's ratio of 0.5, the ν for soft tissue is assumed to be in the vicinity of 0.499.

Thus, we approximate the human soft tissue to be purely elastic, showing linear isotropic behaviour and therefore, characterized by its Young's modulus. The approximated model is solved by finite element method which is explained in the following section.

B. Finite element Modelling(FEM)

The general procedure for solving any continuum mechanics problem involves describing it by a set of relations valid over finite continuous geometric domains and time intervals. Because of the geometrical non-linearities and the complexity of the soft tissue model it is difficult to bring forth analytical solutions defining the system behaviour as a continuous function of time. Thus for the numerical solution, the continuous problem has to be discretized, which is usually implemented using the finite element method (FEM). The solution of the continuous deformation problem is approximated to the solution obtained at the nodes of the mesh which approximates the continuous domain. The FEM is preferred over other numerical techniques because of its flexibility in allowing the analysis of structures with complex geometries with embedded inhomogeneity and boundary conditions. Hence, in this work, we used FEM for modelling the tissue as a linear elastic isotropic solid problem.

C. Geometrical modelling and Numerical simulation

The model (computer phantom) is generated using the finite element analysis software ANSYS *(ANSYS Inc, Canonsberg, PA, USA)* . To study the influence of the applied strain, three categories of a 50 mm X 35 mm rectangular phantom with a rectangular cylindrical inclusion at the depth of 15 mm is modelled. The geometry is shown in Fig.1.(a) which is approximated as a 2D model to be projected on aa' plane. The material properties and dimensions are assigned to the inclusions and background according to the physical composite phantom which we made for experimental analysis. The phantom is modelled as a plane strain, linear isometric elastic problem and meshed with quadrilateral elements of 8 nodes. Compression is simulated as a vertical downward pressure of 5N in y direction which is applied on the top surface of the phantom. The boundary conditions are taken such that it perfectly matches with the experimental set up and hence the lower surface of the phantom is restricted from downward movement and the sides of the rectangles are unconstrained. The nodal and element design of the phantom is shown in Fig.1.(b). The model is solved by a linear solver available in ANSYS. Once the solution is done, the visual display of total mechanical strain can be obtained from the software. The images are represented in color scale where blue represents minimum strain and red indicates maximum strain.

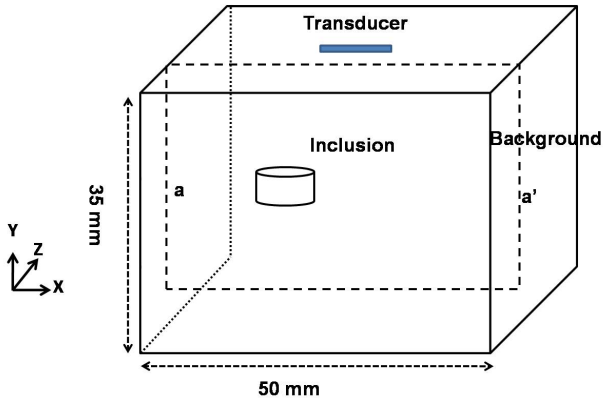

(a) Geometry of the model

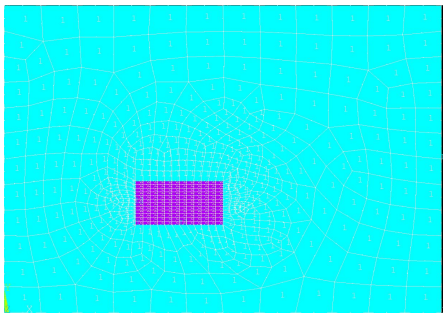

(b) FEM of phantom

Fig. 1: Software model of Phantom

In addition to the computer software phantoms, we have designed, developed and analysed physical agar based composite phantoms for comparing the results. The procedure is explained in the following section.

D. Physical tissue mimicking phantoms

Physical phantoms are developed using hydrogels [4], [5] which are very similar to tissues. In this work, Agar is chosen as the tissue mimicking material. Agar, N-propanol and deionized water are the components of the phantom and they are mixed with correct proportions to match tissue elastic and acoustic properties. Acoustic and elastic properties of the prepared samples are characterised for various concentration

of agar samples using pulse echo ultrasound principle and uni axial compression test on universal testing machine. The preparation procedure and characterisation methods are discussed in our earlier paper [6].

The composite phantom is prepared in three layers. First a thin homogeneous layer in the bottom is prepared with 2 gram of Agar concentration which mimic soft normal tissue. During congealing, holes are made in this homogeneous layer for inserting inclusions. In the next step, holes are filled with varying agar concentration from $4g$ to $8g$. Finally, the whole phantom is covered with the same homogeneous material. The plan and elevation of the composite phantom is shown in Fig.2 (a) and (b). The elastic properties of the background and inclusions are given in table 1. The external view of the prepared phantom is shown in Fig.2 (c).

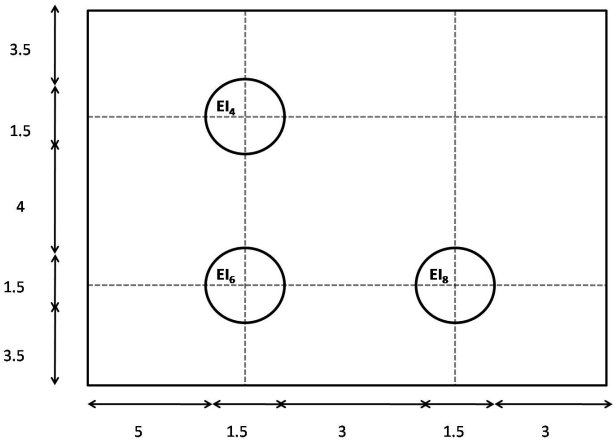

(a) Plan of the phantom

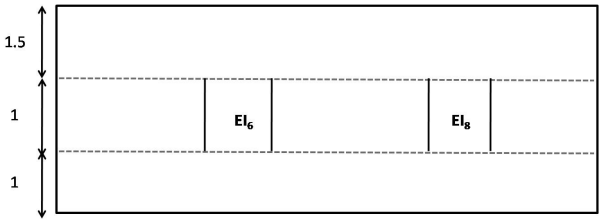

(b) Elevation of the phantom

(c) External view of the composite phantom

Fig. 2: Phantom with inclusions of varying stiffness

TABLE I: Agar Concentration and Elastic Properties of the Composite phantom

Type	Agar Concentration(g)	Young's Modulus (kPa)
Background	2	50
EI_8	8	1000
EI_6	6	300
EI_4	4	180

E. Image Acquisition

Ultrasound B mode and elastograms are acquired using *Siemens S2000* machine at Mediscan Systems, Chennai. Linear array transducer *VF 7-3* with a probe frequency of 5 MHz is used. Phantom is having the dimensions of 14 X 14 X 3.5 cm (length X width X height). Each inclusion is of cylindrical shape having 1.5 cm diameter and 1 cm height. Initially, B mode image of the region of interest (ROI) is obtained with measurements of the inclusion. These measurements are verified with the physical dimensions of the phantom. Once the ROI is highlighted in B-mode image, a slight compression is applied by pressing the transducer on the phantom surface. Built- in software present in the scanner generate the elastogram by comparing the pre-compressed and post-compressed RF signals, and display the elastogram adjacent to the B mode image. Static compressive force around 5N is given by expert radiologist and is measured using a weighing balance placed under the phantom. The weight of the phantom is 660 grams. The elastogram images are displayed along with the B-mode ultrasound images in color scale or gray scale. Color elastogram contains the colors blue- orange- yellow- green- indigo- violet- red with blue representing the regions with no strain (i.e. hardest region) and red representing regions with greatest strain (i.e. softest region).

III. Results and Discussion

The elastogram images of the prepared composite phantom are displayed along with FEM strain images in Fig.3. The Fig.3. a, b and c show the ultrasound, elastogram and FEM strain images for stiff, medium and soft lesions respectively. The ultrasound images are formed based on the reflected back scattering echoes from different interfaces of the phantom. It can be seen that they are not significant in differentiating the inclusion from the background. In contrary, the inclusions are more clear in elastoagram images. The stiff inclusion exhibits no strain compared to the background and the inclusion area is well appreciated in blue color . In case of medium stiff inclusion, the area of inclusion is not uniformly blue, red and green components are introduced, which shows the increased strain. In the case of very soft inclusion, more amount of strain is introduced where we can not get a clear boundary of the inclusion.

The elastogram images are compared with FEM simulated strain images and they have similar patterns. In simulated results, when the stiffness decreases from stiff to soft (Fig.3.a to c), the strain introduced around the inclusion part also increases. Squeezing effect can be seen in the very soft lesion,

where it tries to lose its boundary as seen in the corresponding elastogram image. Elastograms of physical models include noise, where as the results of simulation represent the best image which we can achieve. This result can be taken as an ideal strain image and can be used as a gold standard for signal processing of strain estimation algorithms.

The 2D distribution of strain in the outer areas of the images obtained in the experiment are different from those obtained in simulation. This may be because of the 2D approximation models which we have used here. Moreover uniform meshing is applied for both background and inclusion, since elastogram offers the same resolution to all points under compression. But this may also be a limitation and can be rectified using meshing specific to the local area. In 2D modelling, it does not account the motion in elevational direction. However, the tissue motion under the influence of an external stress is inherently a 3D problem. Therefore the similarity of the resultant simulated strain images can be improved by doing a 3D model of the tissue.

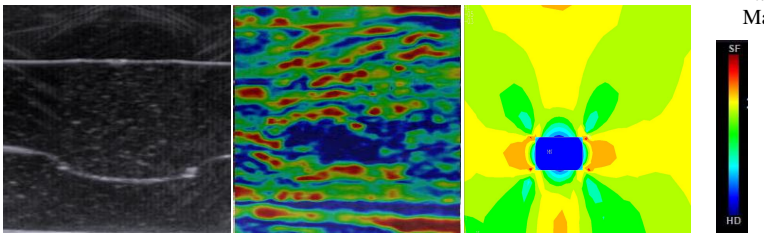

(a)

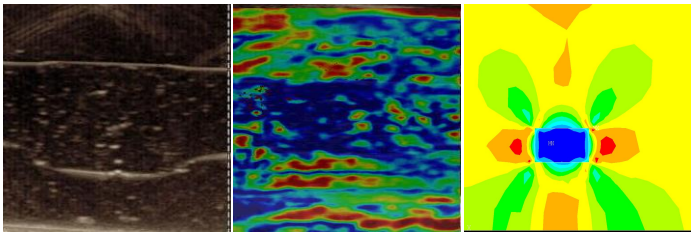

(b)

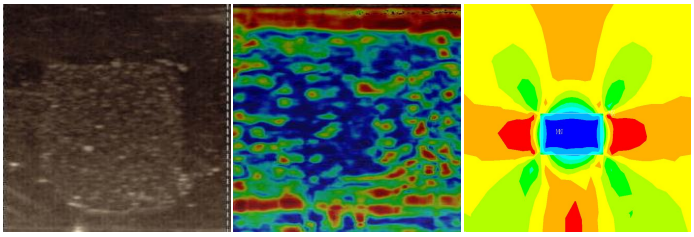

(c)

Fig. 3: a - c Ultrasound B mode (left side), Elastogram (middle) and FEM strain images (right side) of the three embedded inclusions EI_8, EI_6, EI_4 respectively. Elastogram and FEM strain images are represented in color scale. Hardest regions are represented as blue and red color represents soft region as shown in the color bar.

IV. Conclusion

Agar based composite phantoms are developed and their elastic properties are captured using Ultrasound Elastography. The equivalent modelling is also done in finite element method. There is a close similarity between strain images obtained in the physical experiment and the results from finite element analysis. Further enhancement of the result requires conversion from the true strain image of the finite element method into an ultrasound simulated image.

References

[1] Fung.Y.C, *Biomechanics:Mechanical Properties of Living Tissues*. USA: NY, 1993.

[2] Lai.W.M, Rubin.D, and Krempl.E, *Introduction to continuum mechanics.* MA: Butterworth-Heinaman.

[3] Ophir.J, "Elastography:a quantitative method for imaging the elasticity of biological tissues," *Ultrasound Imaging*, vol. 13, pp. 111–134, 1991.

[4] Hall.T.J., Bilgen.M, Insana.M.F., and Krouskop.T.A., "Phantom materials for elastogrpahy," *IEEE transaction on Ultrasound Ferro electronics Frequency control*, vol. 44, p. 1355, 1997.

[5] Madsen.E, Zagzebski.R, Banjavie, and Jutila.P, "Tissue mimicking materials for ultrasound phantoms," *Am. Assoc. Phy. Med.*, vol. 5, pp. 391–394, 1978.

[6] Kavitha.M and RamasubbaReddy.M, "Characterisation of tissue mimicking phantoms for acoustic radiation force impulse imaging," in *Proc. IEEE International Conference on Imaging Systems and Technology (IST2012)*, Manchester, UK, 2012, pp. 553–557.